

1 **Techno-economic assessment of a Multi-effect Distillation plant installed**
2 **for the production of irrigation water in Arica (Chile)**

3
4 Palenzuela, P.^{(1)*}, Miralles-Cuevas, S.^(2,3), Cabrera-Reina, A.^(2,3), Cornejo-Ponce, L.^{(2,3)**}

5 ⁽¹⁾ CIEMAT-Plataforma Solar de Almería, Ctra. de Senés s/n, 04200 Tabernas, Almería, Spain

6 ⁽²⁾ Laboratorio de Investigaciones Medioambientales de Zonas Áridas (LIMZA), Universidad de
7 Tarapacá. Av. General Velásquez 1775, Arica, Chile

8 ⁽³⁾ Escuela Universitaria de Ingeniería Mecánica (EUDIM), Universidad de Tarapacá. Av. General
9 Velásquez 1775, Arica, Chile

10
11 **Corresponding author 1:** Ph.D. Patricia Palenzuela Ardila, (Plataforma Solar de Almería),
12 patricia.palenzuela@psa.es

13 **Corresponding author 2:** Ph.D. Lorena Cornejo Ponce (Universidad de Tarapacá), lorenacp@uta.cl

14
15 **Abstract**

16 In the context of a regional Chilean project (FIC Taltape project, BIP code 30158422-0), a
17 multi-effect distillation (MED) pilot plant has been built and installed in a small community
18 in the north of Chile (Taltape, Arica) in order to supply treated water for agricultural and
19 domestic purposes. The aim of this paper is to assess the techno-economic feasibility of this
20 system for supplying water with the required quality to the population. The characterization
21 of the feed water and the effluents from the MED pilot plant (distillate and brine), obtained
22 during five months of operation, has been firstly performed. Then, the prediction of the
23 operation of the water treatment system with solar energy has been carried out using a typical
24 meteorological year and the design of a static solar field that cover the thermal energy needs
25 of the water treatment plant.

26
27 The annual simulations of the MED pilot plant operating with solar energy showed that the
28 water needs can be mostly covered using a static solar thermal field with a total area of

29 113.2 m², which would generate roughly 46% of the total heat required by the water treatment
30 plant. The technical analysis has been completed with an exhaustive economic assessment.
31 The specific water costs have been determined for the MED pilot plant and the scale factor
32 when the productivity is increased up to 5,000 m³ / day has been evaluated. The cost of
33 distilled water produced by the MED plant varied from 15.0 USD\$/m³ for the 10 m³/day
34 production capacity to 1.25 USD\$/m³ when this variable is increased to 5,000 m³/day.

35

36 **Keywords:** Multi-effect distillation, brackish water treatment, arsenic and boron removal, modelling
37 and simulation, solar thermal water treatment

38

39 **Nomenclature**

R	Retention percentage (%)
C_{BFW}	Concentration of the element in the brackish feed water (mg/L)
C_D	Concentration of the element in the distillate (mg/L)
$\Delta T_{eff,i}$	Temperature difference between effects (°C)
T_v	Vapour temperature inside the effect (°C)
N	Number of effects
Q_s	Heat transfer rate provided to the first effect (kW)
T_s	Temperature of the heating energy source supplied to the first effect
M_s	Steam mass flow rate supplied as the heating energy source to the first effect (kg/s)
λ_s	Change in enthalpy related to the condensation of the steam supplied to the first effect (kJ/kg)
U_e	Overall heat transfer coefficient (kW/m ² ·°C)
M_f	Feedwater mass flow rate (kg/s)

M_{gb}	Total vapour generated inside the effect (kg/s)
λ_{gb}	Latent heat of vaporization (kJ/kg)
C_p	Specific heat (kJ/kg·°C)
T_f	Temperature of the feedwater that reaches the first effect (°C)
M_{prod}	Total distillate obtained from the water treatment plant (kg/s)
RR	Recovery Ratio
sA	Specific area (kg/m ³ /day)
STC	Specific thermal consumption (kWh/m ³)
GOR	Gain Output Ratio
θ	Incidence angle (°)
η_{opt}	Optical efficiency (%)
G_k	Global irradiation over tilted plane (W/m ²)
T_{amb}	Ambient temperature (°C)
\dot{m}	Mass flow rate through the solar collector (kg/s)
T_{col}	Average between the inlet and outlet temperatures of the collector (°C)
T_{in}	Inlet water temperature in the solar collector (°C)
T_{out}	Outlet water temperature in the solar collector (°C)
$K_{\tau\alpha}$	Incident angle modifier
A_a	Aperture area of the collector (m ²)
C_B	Approximate cost of equipment (USD\$)
C_A	Known cost of equipment (USD\$)
S_B/S_A	Ratio known as the size factor
n	Size factor's exponent

$SCOW$	Simplified Cost of Water (\$USD/m ³)
M_W	Annual volume of water produced (m ³)
C_F	Annual fixed costs (\$USD)
C_v	Operating cost (\$USD)
I_o	Initial capital investment (\$USD)
α	Amortization factor
i	Discount rate
t	Depreciation period (year)
$C_{consumables}$	Consumables costs (\$USD)
C_{staff}	Staff costs (\$USD)
$C_{maintenance}$	Maintenance costs (\$USD)
P_e	Total electric power consumed by the MED plant (kW)
N_{col_series}	Number of collectors in series in a row
N_{rows}	Number of rows
N_{total}	Total number of collectors
A_T	Total aperture area (m ²)

40

41 **1. Introduction**

42 Water is a vital resource for both human and economic development, so it is not surprising
43 that the absence or scarcity of water resources is directly related to poverty. Humanity faces
44 a water scarcity problem that grows in a sustained and almost exponential way. According to
45 the World Health Organization (WHO), 844 million people do not have easy access to an
46 improved source of drinking water; furthermore, this number exceeds two billion people if
47 this includes the access to enough water volume (WHO and UNICEF, 2017). This problem

48 is related to governments and institutions around the world, so there are national policies in
49 many countries which aim to achieve universal access to safe water. Two-thirds of the 94
50 countries of the United Nations recognize drinking water and hygiene services as a universal
51 human right and 80% of them have approved national policies in this regard. However, only
52 a quarter of them are carried out as they were established. Despite the remarkable efforts
53 being made worldwide in the field of water, the United Nations institution highlights the
54 fundamental need to increase investment, build human capital and obtain reliable data on
55 which to base global actions (GLAAS Report, 2014).

56 Atacama Desert, which is considered the most arid one in the world, has annually less than
57 10 mm of precipitation per year, presenting isolated areas that only have water coming from
58 rivers and groundwater. Nevertheless, these waters have in many cases a high content of
59 salts, arsenic and boron and, therefore, they are neither suitable for human consumption nor
60 for agricultural and aviculture purposes. This fact limits the development of many locations
61 in the region which only economic resources are selling agricultural products (Bundschuh et
62 al., 2012).

63 The presence of arsenic and heavy metals in the environment is a very acute problem in Latin
64 America (Bundschuh et al., 2010). Arsenic is highly toxic in its inorganic form and its
65 presence is mainly associated with altiplanic quaternary volcanism in the north of Chile.
66 According to the WHO-2016 (WHO, 2016) over 226 million people worldwide are estimated
67 to be drinking contaminated water, with an arsenic contaminant level above the 10 $\mu\text{g/L}$ that
68 WHO establishes as a maximum. This situation can lead to chronic arsenic poisoning
69 (arsenicosis) of which skin lesions and skin cancer are the most characteristic effects
70 (Bhattacharjee, 2013; Hong-Jie et al., 2014; López et al., 2012; Yunus et al., 2011).
71 According to the FONDECYT REGULAR 2011 project results, (FONDECYT REGULAR

72 2011, “An evaluation of the distribution, mobility and bioavailability of the arsenic present
73 in soil and water in the Valley of Camarones, Chile: study of the levels of transference and
74 the accumulation of arsenical species in native plants and crops” Code: 1120881) where an
75 evaluation of the distribution and mobility of the arsenic present in soil and water was
76 performed, the water in the Arica and Parinacota Region presents different levels of arsenic,
77 both As(III) and As(V) species. The highest levels, more than 100 times higher than the levels
78 established by national and international institutions (Decreto Supremo 143/2009; Decreto
79 Supremo 144/2019; Directive 98/83/EC) are found in the Valley of Camarones. This problem
80 presents a difficult solution, as the arsenic cannot be easily destroyed and can only be
81 converted into different forms or transformed into insoluble compounds in combination with
82 other elements, such as iron (Choong et al., 2007).

83 One of the most affected areas in the valley of Camarones is the Taltape community, where
84 the inhabitants economy is mainly based on the exploitation of small agricultural estates,
85 with low-valuable products such as alfalfa, and the production of meat, milk and cheese
86 (mainly from cattle and goats). Due to the above mentioned situation, the generated products
87 contain As and, consequently, these cannot be introduced in the legal markets, which affects
88 the local development. For this reason, there is an important need to solve the water quality
89 problem in a sustainable way so that this location can be established as an agricultural oasis
90 in the middle of the desert, which would allow growing higher added value products such as
91 tomato and/or onion, among others.

92 One of the possible solutions to face up this problem is desalination. Reverse osmosis
93 (RO), multi-stage flash (MSF) and multi-effect distillation (MED) account for more than
94 94% of the worldwide desalination capacity (Li, 2013). The only desalination technology
95 implemented in the Arica and Parinacota Region so far has been RO. However, in spite of

96 its excellent salt rejection characteristics, it presents very low boron and As (III) removal
97 efficiencies (Abejón et al., 2015; Bick et al., 2005; Hilal et al., 2011; Kang et al., 2000;
98 Ning, 2002; Öztürk et al., 2008; Wang et al., 2016). Apart from that, further problems such
99 as red algae blooms make RO desalination more disadvantageous versus the thermal
100 desalination technologies, which are more robust under these particular conditions. The
101 thermal processes also have some other advantages with respect to membrane processes,
102 like: easier operation and maintenance that make their installation possible in countries with
103 lack of experienced personnel, higher purity of the produced distillate and capability to deal
104 with harsh high temperature and salinity feed waters or even with contamination
105 (Palenzuela et al., 2014). Among thermal desalination plants, MED technology is the
106 preferred choice due to its low top brine temperature, typically less than 70 °C, and its low
107 specific energy consumption requirements (Yang and Lior, 2006). On the other hand, the
108 usual coincidence in many locations of fresh water shortage and high isolation levels make
109 the combination of MED processes with solar energy a perfect combination to tackle the
110 water scarcity problem in a sustainable way. Some countries of MENA region (as Qatar,
111 Morocco, etc) and South America (mainly Chile) are more and more promoting the use of
112 solar energy to meet its growing energy and fresh water demands (Darwish et al., 2013;
113 Mohtar and Darwish, 2013; Hanel and Escobar, 2013; Valenzuela et al., 2017).

114 In the context of a regional Chilean project (FIC Taltape project, BIP code 30158422-0), a
115 MED plant to treat brackish water containing As and Boron was installed in the Taltape
116 community. The plant has a fresh water production capacity of 10 m³/day and is driven by
117 thermal energy from a biomass boiler. The electricity required is taken both from a
118 photovoltaic solar field and from a diesel generator (backup). The feasibility of the MED
119 process has been tested with large-scale fossil plants for many years, especially in the Gulf

120 countries. However, there are not many solar MED units in operation. One of the solar MED
121 plants with more operation hours is located at the Plataforma Solar de Almería (PSA). This
122 MED unit presents a freshwater production capacity of 72 m³/day and it is coupled to a static
123 solar field. Several research works have been published in the scientific literature, which
124 analyse the distillate production and the thermal efficiency of this plant at different operating
125 conditions (Fernández-Izquierdo et al., 2012; Palenzuela et al., 2016; Chorak et al., 2017).
126 The best operating conditions to maximize the distillate production found for this plant was
127 to work at the maximum outlet temperature from the solar field and maximum value of the
128 feed water flow rate in summer months and at minimum vapour temperature in the condenser
129 and maximum outlet temperature from the solar field in winter months (Chorak et al., 2017).
130 There is another solar MED plant located in Abu Dhabi, which is one of the first plants to be
131 installed (120 m³/day capacity) (El-Nashar and Ishii, 1985), although not much data have
132 been reported from its operation. Only one test campaign developed in this solar MED plant
133 has been published in the literature and it was focused on the validation of a steady-state
134 model (El-Nashar and Qamhiyeh, 1995). The results showed that the product water flow rate
135 increased from 4 to 7 m³/h with the increase in the heating water temperature and it remained
136 almost constant with the change in the heating water flow rate. On the other hand, it was
137 observed that the specific heat consumption increased from 40 to 50 kcal/kg distillate when
138 the heating water temperature rose from 65 to 75 °C. As far as the authors' knowledge, there
139 are no techno-economic studies in the scientific literature that address the use of MED plants
140 with solar energy to obtain treated water for agricultural purposes.

141 The goal of this study case is to carry out a techno-economic assessment of a MED plant with
142 eight effects to treat brackish water from Camarones River located in Taltape (Arica and
143 Parinacota Region, Chile), which presents high As and Boron content, for agricultural and

144 domestic purposes. For the technical analysis, an initial characterization of the feed water
145 and the effluents from the MED plant (distillate and brine) obtained during several months
146 of operation, has been performed. Then, a design model of the MED plant has been developed
147 and implemented in Matlab with simulation purposes. The plant is currently coupled to a
148 biomass boiler that provides the thermal energy required to operate the MED plant and to a
149 photovoltaic solar field and a diesel generator (as back-up) for the electricity requirements of
150 the distillation plant. The biomass boiler will be replaced by a thermal static solar field that
151 is sized in the present work as the main element to provide the thermal energy to the MED
152 plant, using the boiler as a backup when the solar energy is not available. Moreover, the
153 thermal static solar field has been designed and a model of this field that predicts the hourly
154 thermal power provided to the MED unit along the year has been developed using a typical
155 meteorological year. This model also determines the annual solar fraction, which is the
156 relation between the amount of energy obtained through the used solar technology and the
157 total annual energy required by the process. Finally, the annual freshwater production has
158 been determined and an economic analysis has been performed including the plant scale in
159 order to provide different amounts of fresh water up to 5,000 m³ / day.

160 **2. Description of the system installed**

161 **2.1. Multi-Effect Distillation plant**

162 The MED pilot plant of Taltape (see the flow diagram in Fig. 1), manufactured and delivered
163 by INERCO Tratamiento de Aguas S.A. (Madrid, Spain) in 2016 consists of simultaneous
164 evaporation processes of brackish water and subsequent vapour condensation at decreasing
165 pressures and temperatures from the first effect to the last one. This plant has eight effects
166 and each one consists in a submerged tube heat exchanger provided by AURUM Processes
167 Company (Murcia, Spain), through which steam flows as thermal energy source. The

168 brackish water comes from the Camarones River and is firstly collected in a reserve tank
169 (RT1, 10 m³) and pre-treated by microfiltration (25µm cartridge filter) before starting the
170 distillation process. From RT1, water is pumped to the MED plant (24.3 m³/h). Among the
171 total flow rate, 23 m³/h are pumped to the end condenser for refrigeration and 0.8 m³/h of
172 feed water (pre-treated in a sand filter) is sent to the first effect of the MED plant after flowing
173 through the preheaters. The remaining flow rate (0.5 m³/h) is used to cool down the vacuum
174 pump (VP1) working on the brackish water circuit (see Fig. 1). Another vacuum pump (VP2)
175 is cooled by the distillate water circuit. These two vacuum pumps are used to discharge the
176 brine and the distillate outside the plant, also providing the necessary vacuum conditions in
177 the process.

178 The first effect is heated with hot water coming from a biomass boiler (20 m³/h, 70°C). The
179 brackish water enters the first effect passing through all the pre-heaters and part of it is
180 evaporated generating steam that is later used as the thermal energy source for the following
181 effect. The brackish water that has not been evaporated in the first effect (called brine), goes
182 to the second effect where there is partially evaporated by the steam entering the second
183 effect that transfers its latent heat to the brine. The steam is then condensed, being the first
184 distillate of the process. In order to maximize the energetic efficiency of the plant, this
185 condensate enters the next effect along with the steam that has been already produced in the
186 previous effect. The same process is repeated for the rest of effects.

187 The extraction of the distillate and brine is obtained by means of two vacuum pumps (VP 1
188 and 2), one for each circuit. In order to facilitate the extraction of both streams, two small
189 reservoir deposits (0.2 m³) were installed, one for each stream. When these reservoirs
190 accumulate enough volume, the distillate/concentrate is extracted by the corresponding pump
191 to another reservoir tank (RT 2, 5 m³). Later, in a third reservoir tank (RT3, 10 m³) the

192 produced distillate water is post-treated to achieve irrigation and domestic water
 193 characteristics (post-treatment). Finally, the brine is mixed with the outlet of the cooling
 194 stream and returned to the Camarones River (see Fig. 1). Notice that the brine represents only
 195 1- 2% of the total waste volume, so the mixture that finally is spilt into the river does not
 196 damage the ecosystem.

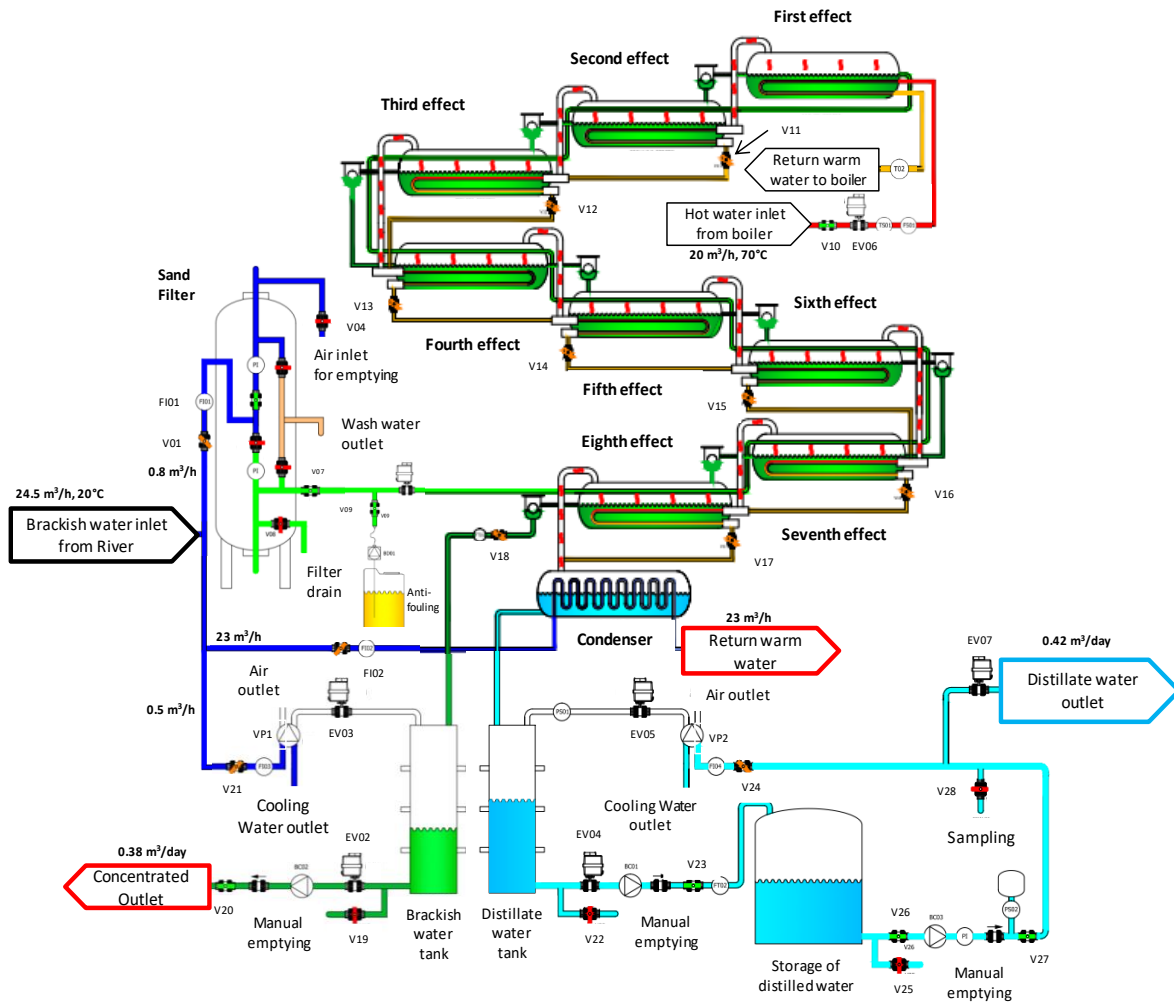


Fig. 1. Scheme of MED system

197

198 2.2 Energy supply systems

199 The energy supply, electricity and thermal energy, for the MED plant is done by a
 200 photovoltaic (PV) solar field and a diesel generator for the electricity requirements and by a

201 biomass boiler for the thermal energy requirements. Fig. 2 shows a scheme of how the
202 installed MED unit is coupled to the mentioned energy supply systems. The PV solar field
203 consists in 10 PV panels of polycrystalline silicon. The panels are tilted 19° (local latitude).
204 The dimensions of each panel are 1,640x990x40 mm with 60 cells per panel. The total surface
205 is 15.8 m^2 with 3.1 kW_p (P_{max} per panel = 320W). Four stationary batteries of Lithium 12V
206 250 AH are available in the system. The Diesel generator was provided by VIELCO
207 Company, KIPOR PRO-X model KDS28SS3. It has an output of 21.3 kVA (17 kW) and
208 works at 1500 rpm with $\cos\Phi= 0.8$, at 230 or 400 V. The necessary electricity for the whole
209 system (MED production of $10 \text{ m}^3/\text{day}$) is considered as 12 kW corresponding to: (i) MED
210 plant (5 kW), (ii) 4 pumps outside (3 x 2 kW and 1 x 0.5 kW) and (iii) the boiler (0.5 kW).
211 The electricity is provided only by the PV system during the sun hours and diesel generator
212 is used as backup during the night.

213 The biomass boiler was provided by Nueva Energía, Biocalora serie 2000 model B-MAX 50.
214 It has a rated thermal input of 50 kW and the heating surface is between $600 - 900 \text{ m}^2$, being
215 fuel type pellets DIN $\varnothing 6 \text{ mm} \div L = 5 - 30 \text{ mm}$. The boiler performance is 90.1% with 2 bars
216 of pressure max and $90 \text{ }^\circ\text{C}$ of maximum operation temperature.

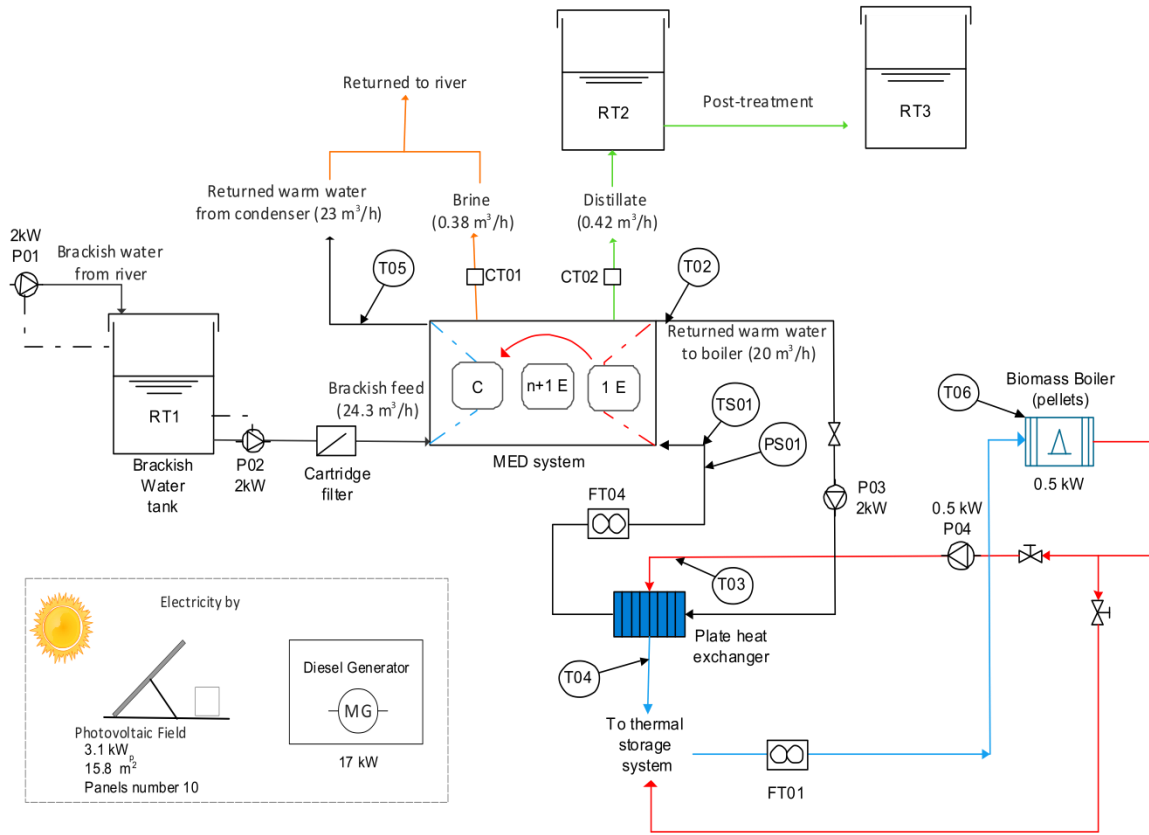


Fig. 2. General scheme of system

217

218 3. Techno-economic assessment

219 3.1 MED's effluents characterization

220 The characteristics of the brackish feed water from Camarones River and the effluents
 221 obtained from MED operation (brine and distillate) were gathered during several months.
 222 Average values are shown in Table 1 (the parameters of the waste stream returned to
 223 Camarones River were calculated by mass balance).

224 In order to determine the percentage of solutes remaining in the brine solution, the retention
 225 percentages are determined by Eq. 1. The results are shown in Table 1:

$$R(\%) = \frac{C_{BFW} - C_D}{C_{BFW}} \cdot 100 \quad (1)$$

226 where C_{BFW} is the concentration of the corresponding parameter (As, B, Cd, Cu, etc.) in the
 227 brackish feed (mg/L) water and C_D the same one in the distillate water (mg/L).

228 Notice that all the retention percentages obtained were higher than 90% and more specifically
 229 B and As, that were removed in 95% and 99% respectively. As explained above, these are
 230 especially toxic elements for plants and humans, respectively.

231 **Table 1**
 232 Characterization of brackish feed water, brine, distillate and waste stream

	Units	Brackish feed water	Brine	Distillate	R (%)	Waste stream (refrigeration + brine)
Flow	m ³ /h	0.80	0.38	0.42	--	23.38
Total Dissolved Solids (TDS)	mg/L	1,900	3,980	19.0	99	1,930
Conductivity	μS/cm	2,600	5,250	200	92	2,640
Arsenic (A _{total})	mg/L	0.60	1.26	0.006	99	0.61
Boron (B _{total})	mg/L	15.0	30.8	0.75	95	15.2
Cadmium (Cd ⁺²)	mg/L	0.05	0.10	0.004	92	0.051
Calcium (Ca ⁺²)	mg/L	210	430	8.4	96	213
Chlorides (Cl ⁻)	mg/L	700	1,420	49.0	93	711
Copper (Cu ⁺²)	mg/L	0.05	0.10	0.001	99	0.051
Iron (Fe _{total})	mg/L	0.20	0.40	0.016	92	0.20
Magnesium (Mg ²⁺)	mg/L	25.0	52.0	0.25	99	25.4
Manganese (Mn ⁺²)	mg/L	0.13	0.27	0.003	98	0.13
Plumb (Pb ⁺²)	mg/L	0.03	0.06	0.003	91	0.030
Potassium (K ⁺)	mg/L	35.0	72.0	1.8	95	35.6
Selenium (Se _{total})	mg/L	0.20	0.41	0.01	95	0.20
Sodium (Na ⁺)	mg/L	200	420	2.0	99	203
Sulphates (SO ₄ ²⁻)	mg/L	310	625	24.8	92	315
Zinc (Zn ⁺²)	mg/L	0.30	0.62	0.006	98	0.31

233

234 **3.2. Modelling and scale up of the solar water treatment system**

235 **3.2.1 MED plant**

236 Taking the MED pilot plant located at the Taltape community as reference (8 stages, 10
 237 m³/day), a scale-up has been carried out for higher capacities, from 10 m³/day to 5,000
 238 m³/day, in order to perform the economical assessment later. For this purpose, a design model

239 of a MED plant with the same configuration as the one implemented in Taltape has been
 240 developed and implemented in Matlab. The MED model is based in the one published in
 241 (Palenzuela et al., 2014) but particularized for this study. In this model, unlike that the one
 242 described in our previous work, equal area in all effects was considered. For the computation
 243 of the model, an iteration loop was implemented in the Matlab software that starts with the
 244 temperature profile and continues until a convergence criterion is achieved. The convergence
 245 criterion of the model should have a maximum difference in effect areas of $1 \cdot 10^{-4}$ in order to
 246 achieve a good accuracy.

247 Firstly, the temperature difference between effects is obtained by the following equation:

$$\Delta T_{eff,i} = \frac{T_{v,1} - T_{v,N}}{N - 1} \quad (2)$$

248 where N is the number of stages, $T_{v,1}$ is the vapor temperature generated in the 1st effect and
 249 $T_{v,N}$ is the vapor temperature generated in the last effect. In all cases, N has been established
 250 as 8 stages, $T_{v,1}$ as 70 °C and $T_{v,N}$ as 35 °C.

251 On the other hand, the area of each evaporator (A_{ei}) is defined by the heat transfer equation.
 252 For the sake of simplicity, all the equations shown correspond to the first effect but can be
 253 extrapolated to the rest of effects:

$$Q_s = A_{e1} U_{e1} (T_s - T_{v1}) = M_s \lambda_s \quad (3)$$

254 where Q_s is the heat transfer rate provided to the first effect, T_s the temperature of the heating
 255 energy source supplied to the first effect of the MED plant, T_{v1} is the temperature of the
 256 vapor generated inside the first effect, M_s is the steam mass flow rate supplied as the heating
 257 energy source to the first effect, λ_s is the change in enthalpy related to the condensation of
 258 the steam supplied to the first effect, and U_{e1} is the overall heat transfer coefficient of the

259 first evaporator. Notice that, although the heat transfer source provided to the first effect in
260 the MED pilot plant of Taltape is hot water, for the high scale MED plants, steam has been
261 considered as the energy source to match the commercial plants worldwide.

262 The overall heat transfer coefficient is determined by the correlation proposed by El-
263 Dessouky and Ettouney (2002):

$$U_{e1} = 1.9695 + 1.2057 \cdot 10^{-2}T_{v1} - 8.5989 \cdot 10^{-5}T_{v1}^2 + 2.5651 \cdot 10^{-7}T_{v1}^3 \quad (4)$$

264 The ratio between the sum of all the evaporator areas to the distillate production is called
265 specific area (**SA**) and it is a characteristic parameter that gives an idea of the size of the MED
266 plants.

267 The mass flow rates of distillate and brine together with the temperatures of all the streams
268 are determined by mass and energy balances in all the effects:

$$M_f = M_{gb,1} + M_{b,1} \quad (5)$$

269 where $M_{gb,1}$ is the total vapor generated that, in turn, is converted to distillate when it
270 condenses in the following effect, M_f is the feedwater mass flow rate and $M_{b,1}$ is the brine
271 flow rate that remain from the evaporation taking place in the first effect.

$$M_{gb,1}\lambda_{gb,1} = M_s\lambda_s - M_f C_p (T_{v1} - T_f) \quad (6)$$

272 where $\lambda_{gb,1}$ the latent heat of vaporization at T_{v1} , C_p is the specific heat and T_f the
273 temperature of the feedwater that reaches the first effect of the MED plant.

274 One of the parameters that evaluates the performance of the MED plant is the Recovery Ratio
275 (**RR**), which is defined as the ratio of the total distillate obtained from the plant (M_{prod}) to
276 the feed water flow rate (M_f):

$$RR = \frac{M_{prod}}{M_f} \quad (7)$$

277 This parameter has been established as an input in the model of the MED plant and a value
 278 of 50% has been considered in all cases (this is a fair value when low salinity feed water is
 279 being treated by an MED plant).

280 Another performance parameter is the specific thermal consumption (**STC**), which is defined
 281 as the thermal energy supplied to the plant (Q_s) for the total distillate obtained from the plant:

$$STC = \frac{Q_s}{M_{prod}} \quad (8)$$

282 The third performance parameter of this kind of plants is the Gain Output Ratio (**GOR**) which
 283 is defined as the mass flow rate of distillate produced per consumed heating steam rate:

$$GOR = \frac{M_{prod}}{M_s} \quad (9)$$

284

285 **3.2.2. Thermal solar field**

286 The thermal solar field has been sized for all the sizes of the MED plant (from 10 m³/day to
 287 5,000 m³/day) and the results in terms of total aperture area have been used in the economic
 288 assessment. It has been considered as a solar field composed by evacuated tube collectors
 289 (ETC) to supply the thermal energy required by the MED plant, since they are the ones with
 290 the highest efficiency among the static solar collectors. The selected collector is from the
 291 company sunflower renewable energy Co. (model SF-BF305818) whose technical
 292 characteristics are shown in Table 2.

293 **Table 2**

294 Characteristics of the ETC (results of EN 12975 test results)

Aperture area: 2.83 m²

Longitudinal incidence angle modifier	$\theta_L=10^\circ$: 1.00
	$\theta_L=20^\circ$: 1.00
	$\theta_L=30^\circ$: 0.99
	$\theta_L=40^\circ$: 0.97
	$\theta_L=50^\circ$: 0.92
	$\theta_L=60^\circ$: 0.84
	$\theta_L=70^\circ$: 0.68
Tangential incidence angle modifier	$\theta_T=10^\circ$: 1.04
	$\theta_T=20^\circ$: 1.09
	$\theta_T=30^\circ$: 1.23
	$\theta_T=40^\circ$: 1.38
	$\theta_T=50^\circ$: 1.78
	$\theta_T=60^\circ$: 1.82
	$\theta_T=70^\circ$: 2.08
Efficiency parameters	η_{opt} : 0.64
	c_1 : 1.494 W/ K·m ²
	c_2 : 0.012 W/ K ² ·m ²
Flow rate: 0.020 kg/s·m ²	

296 η_{opt} , c_1 and c_2 are the optical efficiency and the coefficients accounting for thermal losses,
297 respectively.

298 The collectors are orientated to the North and with a tilt angle equal to the local latitude. The
299 location of Taltape has the following geographical coordinates: lat. 18.99° S, long. 69.77°
300 W. For the size of the solar field, a design point (specific date, including month, day and
301 time) is firstly selected from a typical meteorological year (TMY) that has been obtained
302 with Meteonorm software for the specific location. The design point selected has been 19th
303 of June at solar noon (this time corresponds to sun zenith and presents greater stability of the
304 direct solar irradiation) due to the good weather conditions, which can lead to higher solar
305 operation hours of the water treatment plant. Also, a solar multiple of 2 has been considered
306 in order to have an annual solar contribution close to 50% (it means higher hours of solar
307 operation for the water treatment system).

308 Table 3 shows the monthly data of global irradiation over tilted plane (G_k) and ambient
309 temperature (T_{amb}).

310 **Table 3**
311 Data of irradiation and ambient temperature of a TMY in Taltape, Arica

Month	G_k [kWh/m ²]	T_{amb} [°C]
January	190	19.9
February	173	20.2
March	188	19.4
April	154	16.9
May	136	14.2
June	110	12.4

July	119	11.9
August	137	11.9
September	154	12.6
October	180	14.3
November	186	16.1
December	186	18.2

312

313 The global irradiation data has been normalized with the actual measurement of the yearly
314 global irradiation over a tilted plane (G_k , 2,110 kWh/m²·y) obtained from a radiometric
315 measuring solar station located close to the selected location.

316 The design of the solar field is carried out by firstly determining the number of collectors in
317 series in a row and secondly the number of rows in parallel.

318 On one hand, the number of collectors in series in a row is determined by the ratio between
319 the temperature increase required in a row and the temperature step of an individual solar
320 collector. The outlet temperature reached at the outlet of the collector is determined by the
321 efficiency equation of the collector:

322

$$\eta_i = \frac{\dot{m}C_p(T_{out} - T_{in})}{G_k A_a} = \eta_{opt} K_{\tau\alpha} - c_1 \left[\frac{(T_{col} - T_{amb})}{G_k} \right] - c_2 \left[\frac{(T_{col} - T_{amb})^2}{G_k} \right] \quad (10)$$

323

324 where \dot{m} is the heat transfer fluid (i.e. water) mass flow rate through the solar collector; C_p
325 is the average heat capacity of the heat transfer fluid; T_{col} is the average between the inlet
326 and outlet temperatures of the collector; T_{in} and T_{out} are the inlet and outlet temperatures in

327 the solar collector, respectively; G_k is the global solar irradiance on tilted plane in W/m^2 , A_a
328 is the aperture area of the collector and $K_{\tau\alpha}$ is the incident angle modifier, which is
329 determined as the product between the longitudinal and tangential incident angle modifiers
330 (see Table 2):

$$K_{\tau\alpha} = K_{\tau\alpha}(T) \cdot K_{\tau\alpha}(L) \quad (11)$$

331 Considering the operational temperature of the MED plant between 65 °C and 75 °C, a
332 temperature increase in the solar field from 75 °C to 85 °C has been established for the
333 calculation.

334 On the other hand, the number of rows is determined as the ratio between the thermal power
335 to be supplied by the solar field (that is the thermal power required by the MED plant, which
336 is defined by the specific thermal consumption and distillate production of the plant) and the
337 thermal power supplied by one individual row. This last one is determined from the thermal
338 power supplied by one collector (according to equation 10), multiplied by the number of
339 collectors connected in series. The product of the number of collectors connected in series
340 and the number of rows gives the total number of collectors required by the solar field that
341 multiplied by the aperture area of one collector, leads to the total area of the solar field.

342 Finally, an annual simulation model of the dimensioned solar field developed by the authors
343 (Andrés-Mañas et al., 2017) has been used to determine the hours of operation of the water
344 treatment plant with solar energy for all MED plant capacities. The model determines the
345 thermal power supplied by the solar field every hour by an iteration loop that recalculates the
346 flow rate through the solar field as a function of the outlet temperature reached. The hours of
347 solar operation are considered when the hourly power provided by the solar field is higher
348 than the 50% of the MED thermal load. The model also gives the solar fraction, which is

349 defined as the relation between the amount of energy obtained through the solar technology
350 used and the total annual energy required by the process. The amount of energy obtained
351 through the solar technology is determined as the sum of the thermal power provided in each
352 interval multiplied by the time interval, and the total energy required by the process as the
353 thermal power multiplied by the hours of operation and by the total days in the year. Also,
354 the model gives the annual fresh water produced by the MED plant with the thermal energy
355 provided by the solar field. The definition of Gain Output Ratio has been used for this
356 purpose.

357 **3.3 Economical assessment**

358 The economical assessment was done using the data obtained from the plant installed at
359 Taltape (10 m³/day), which includes actual data about the system implementation and
360 operation. The plant scaling up was carried out up to 5000 m³/day, which is considered the
361 water production needed to supply the nearest city located at the same Chilean region as
362 Taltape, named Arica, with approximately 200,000 inhabitants. For the evaluation of the
363 scaling up effect, 10, 200, 500, 1,000, 2,500 and 5,000 m³/day have been taken as the
364 production capacities. In addition, 350 operating days per year were taken into account,
365 corresponding to a water production of $3.5 \cdot 10^3$ m³/yr for the smallest MED plant and
366 $1.75 \cdot 10^6$ m³/yr for the biggest MED plant considering a 24/7 operating regime. According to
367 (Papapetrou et al., 2017), it is necessary to define boundary conditions for the cost
368 calculation. In this work, post-treatment of distilled water is excluded as well as water
369 distribution, laboratory for quality control and distillation plant decommissioning at the end-
370 of-life. Chemical costs included in the calculation were (industrial-grade prices obtained
371 from Chilean companies): pellets for biomass boiler 0.17 USD\$/kg -price provided by
372 PROENERGY S.L. (VIII region, Chile); Diesel for generator 0.63 USD\$/L -price provided

373 by PETRONOR S.L. (XV region Chile); Oil and refrigerant for maintaining of generator
 374 motor was 7.2 and 7.4 USD\$/L, respectively -prices provided by SODIMAC S.L. (XV
 375 region, Chile); anti-fouling model GMP 670 was 8.7 USD\$/L -prices provided by GENESYS
 376 MEMBRAM PRODUCTS (Metropolitan region, Chile)-.

377 For the scaling of the main equipment, the costs can be obtained by the Rule of Six Tenths
 378 (Seider et al. 2004) if the cost of a similar item of different size or capacity is known. The
 379 following equation, Eq. 12, expresses the rule of six-tenths:

$$C_B = C_A \cdot \left(\frac{S_B}{S_A}\right)^n \quad (12)$$

380 where C_B represents the approximate cost (USD\$) of equipment having size S_B (kW, Hp, m²,
 381 or whatever). C_A is the known cost (USD\$) of equipment having a corresponding size S_A
 382 (same units as S_B), and $\frac{S_B}{S_A}$ is the ratio known as the size factor, dimensionless. The size
 383 factor's exponent, "n", depends on the equipment type and it can vary from 0.3 to 1 with an
 384 average value near 0.6 (see Table 4) (Couper, 2002).

385 **Table 4**
 386 Size factor, interest and period of amortization

Main equipment	Size factor's exponent (n)	Interest rate (i, %)	Depreciation period (t, years)
MED	0.53	5	20
Biomass boiler	0.50	5	10
Diesel generator	0.60	5	5
Solar fields (thermal and PV)	0.60	5	15

387

388 The water treatment costs are calculated by the Simplified Cost of Water (SCOW) method
 389 (Papapetrou et al., 2017) using Eq.13.

$$SCOW = \frac{C_F + C_v}{M_w} \quad (13)$$

390 where M_w is the annual volume of water produced, C_F the annual fixed costs and C_v operating
391 costs.

392 The annual fixed costs (Eq. 14) include the construction of the plant (amortization of the
393 equipment and material), engineering, construction and project management, initial design
394 and permitting and land cost (Papapetrou et al., 2017). According to (Papapetrou et al., 2017),
395 normally, most of these costs are ignored and these are presented as an approximated
396 percentage of the main equipment costs. In this case, the initial design, engineering,
397 construction and project management costs were considered to be included in the MED plant
398 facility cost as it was provided by INERCO Tratamiento de Aguas S.A. In addition, the
399 Municipality of Camarones handed over the land and gave the corresponding permissions
400 free of charge. Normally, the cost of land is never considered as it greatly depends on the
401 plant geographical location.

402

$$C_F = \sum I_o \cdot \alpha \quad (14)$$

$$\alpha = \left(\frac{i}{1 - (1 + i)^{-t}} \right) \quad (15)$$

403

404 where I_o is the initial capital investment, α the amortization factor, i is discount rate and t is
405 depreciation period in years.

406 On the other hand, the variable costs (or operating costs) (Eq. 16) include: reagents and
407 chemical consumptions ($C_{consumables}$), energy needed, staff (C_{staff}) and maintenance of the
408 facility ($C_{maintenance}$). Regarding the energy needed, electricity consumption was not
409 considered as operating cost because there is no electric network available in the Taltape
410 community (as already mentioned, a diesel generator is used to supply the electric energy

411 when solar radiation is not available). In this way, the diesel and pellet consumptions used to
 412 generate on-site energy are considered within the operating costs ($C_{consumables}$), while the
 413 diesel generator and boiler were considered as main equipment in the annual fixed costs.

$$C_v = (C_{consumables} + C_{staff} + C_{maintenance}) \quad (16)$$

414

415

416

417 **4. Results and discussion**

418 **4.1. Dimensioning of the MED and solar thermal field**

419 Table 5 shows the results obtained from the design of the MED plant for distillate productions
 420 of 200, 500, 1,000, 2,500 and 5,000 m³/day. As shown in the Table 5, the GOR obtained was
 421 6.9 considering MED plants of 8 stages and a temperature lift (temperature difference
 422 between the vapor temperature inside the first and last effects) of 35 °C. As expected, the
 423 thermal power required by the distillation process increases proportionally with the plant
 424 capacity. These values were used to scale up the kW_{th} needed in the biomass boiler and the
 425 kW_e needed in the diesel generator.

426 **Table 5**

427 Results from the design of the MED plant with different distillate production. All the
 428 variables are described in the nomenclature

	200	500	1,000	2,500	5,000
	m ³ /day	m ³ /day	m ³ /day	m ³ /day	m ³ /day
Q_s (kW _{th})	775	1937.5	3,875	9,687.5	19,375
M_s (kg/s)	0.4	0.8	2.0	3.3	8.0
GOR	6.9	6.9	6.9	6.9	6.9
M_f (m ³ /h)	18	38	100	165	400

A_{ef} (m ²)	74	170	427	705	1,708
P_e (kW _e)*	18.3	45.8	91.7	229.2	458.3

429 * P_e is the total electric power consumed by the MED plant, which has been determined assuming a specific
430 electric consumption of 2.2 kWh/m³ for all cases.

431

432 Regarding the solar thermal field, Table 6 shows the results corresponding to the pilot plant
433 installed in Taltape. The resulting solar thermal field is formed by 40 ETC with a total
434 aperture area of 113.2 m² and an outlet temperature from a solar collector of 88.1 °C.

435 **Table 6**

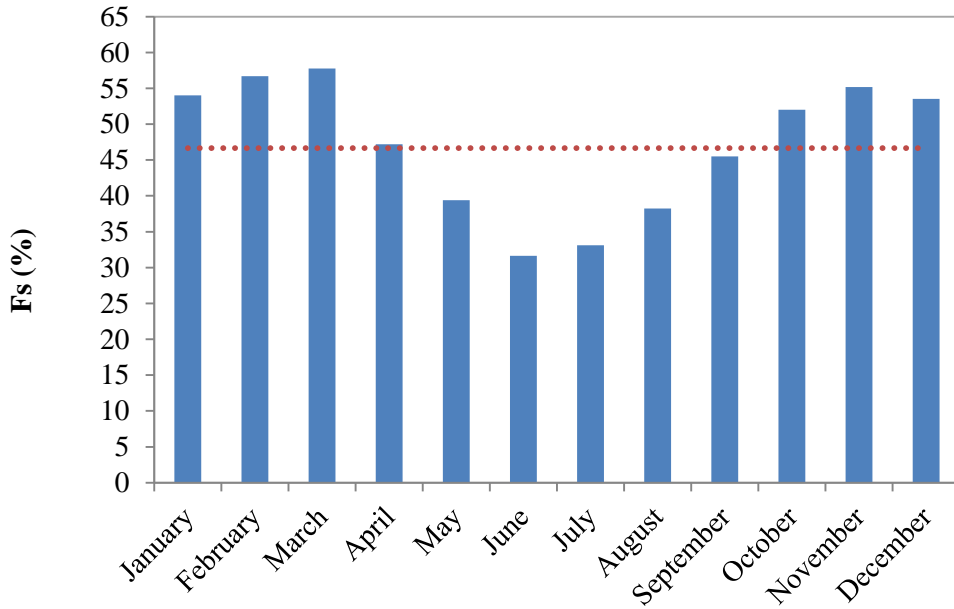
436 Solar thermal field dimensioning results for the pilot MED plant located in Taltape

Variables	Values
T_{out}	88.1 °C
N_{col_series}	1
N_{rows}	40
N_{total}	40
A_T	113.2 m ²

437

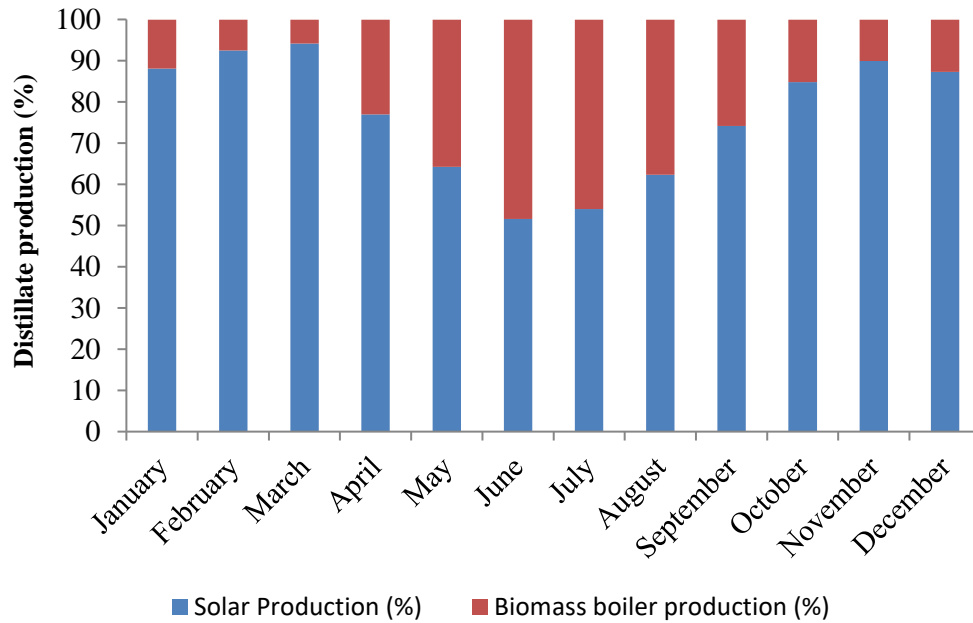
438 In order to have a better representation of the behavior of the MED pilot plant located at
439 Taltape with the solar field and biomass boiler, monthly simulations have been performed to
440 determine the solar fraction (F_s) and the fresh water produced every month. The results are
441 represented in Fig. 3. The highest solar fraction was obtained in March, 57.8%, which nearly
442 doubled the solar fraction of the worst month, June, with 31.6%. The annual average solar
443 fraction was 46.6%, which is represented in Fig. 3 as a dotted line, and the annual energy
444 provided by the solar field was 560.9 GJ.

445



446
 447 **Fig. 3.** Monthly solar fraction in Taltape, Arica (blue bars) and annual average solar
 448 fraction (red dotted line).

449
 450 The ratio between the monthly fresh water produced by solar energy and the monthly fresh
 451 water demanded and the same ratio but with the monthly fresh water produced by the biomass
 452 boiler (red bars) has been determined in order to have an idea of the solar operation of the
 453 MED plant (see Fig. 4). The fresh water demanded is the amount of drinking water, domestic
 454 and hygiene use established by UNESCO. As expected, the MED plant will operate mostly
 455 with solar energy during summer and spring months (January, February, March, October,
 456 November and December), covering between 85-95% of the freshwater only with solar
 457 energy. During autumn and winter months (from April to September), the percentage of use
 458 of the boiler is higher, reaching a percentage of nearly 50% in June. From the annual
 459 simulation, a total fresh water production with the MED operating with the thermal energy
 460 provided by the solar field of 1,690 m³ was obtained, which means a total of 2,823 hours of
 461 solar operation.



463

464 **Fig. 4.** Relative fresh water production with respect the water demand established by
 465 UNESCO, using solar thermal energy (blue bars) and using the biomass boiler (red bars)
 466 along the year.

467 For the rest of cases (the scales-up to higher fresh water capacities), Table 7 shows the size
 468 of the solar thermal field in terms of total number of collectors (N_T) and total aperture area
 469 (A_T), the annual thermal energy provided by the solar field (E_{SF}), the annual fresh water
 470 produced by solar energy (F_{sw}) and the annual hours of solar operation (H_{op}) of the MED
 471 plant. As can be seen, the solar fraction and hours of operation are kept almost constant in all
 472 cases. The rest of parameters are increased in the same scale factor as the capacity (2.5).

473

Table 7

474

Results from the dimensioning of the solar thermal field and from the annual simulation of
 475 the solar water treatment system

MED						
capacities (m^3/day)	N_T	A_T	F_s (%)	E_{SF} (GJ)	F_{sw} (m^3)	H_{op} (h)
200	838	2372	48.9	$1.2 \cdot 10^4$	$3.5 \cdot 10^4$	2861
500	2100	5943	49.0	$3.0 \cdot 10^4$	$8.9 \cdot 10^4$	2863

1000	4202	11892	49.0	$6.0 \cdot 10^4$	$1.8 \cdot 10^5$	2864
2500	10504	29726	49.0	$1.5 \cdot 10^5$	$4.4 \cdot 10^5$	2864
5000	21006	59447	49.0	$3.0 \cdot 10^5$	$8.9 \cdot 10^5$	2864

476

477 **4.2. Economical assessment**

478 The initial capital costs (I_0 in USD\$) accounting for the MED plant, which correspond to the
479 biomass boiler, the diesel generator (installed elements) and the solar thermal and
480 photovoltaic fields are shown in Table 8, together with the annual fixed costs (C_F both in
481 USD\$ and USD\$/m³). These costs include the actual values paid to the supplier companies
482 that participated in this initiative (INERCO Tratamiento de Aguas S.A. Madrid, Spain –MED
483 plant-, VIELCO Company –diesel generator- and Nueva Energía –boiler- and
484 SOLUTECHNO, Perú –solar photovoltaic fields-) and a quotation provided by
485 SOLUTECHNO, Perú, according to the results obtained from the size of the solar thermal
486 field. Then, the investment costs for the 10 m³/day size plant are: 579 USD\$/m² for the solar
487 thermal installation including storage, 8.0 USD\$/W_p, 9,400 USD\$ for the diesel generator
488 and 11,600 USD\$ for biomass boiler and an initial capital cost of 139,900 USD\$ for the water
489 treatment unit (MED). Assuming the amortization periods and interest rates shown in Table
490 4, the annual fixed cost for the main equipment of the system can be calculated. Notice that
491 only the cost variation caused by the plant scaling up from 10 m³/day to 200 m³/day is
492 analyzed in detail in this section in order to simplify the discussion (see Tables 8 and 9).
493 Thus, Table 9 shows the breakdown of the operating costs for the MED plant installed (10
494 m³/day) and scaled up (200 m³/day). When calculating the SCOW, the results are shown in
495 Table 10 for all water treatment capacities considered in this study (from 10 to 5,000 m³/day).

496

497 **Table 8**

498 Initial capital costs (I_0) and annual fixed costs (C_F) for the main equipment

Treatment capacity		MED plant	Biomass boiler	Diesel generator	Solar thermal and PV fields	Total
10 m ³ /day	I ₀ (USD\$)	139,900	11,600	9,400	90,500	251,400
	C _F (USD\$)	11,200	1,500	2,200	8,700	23,600
	C _F /M _w (USD\$/m ³)	3.2	0.4	0.6	2.5	6.7
	Relative cost (%)	47.5	6.1	8.9	35.4	-
200 m ³ /day	I ₀ (USD\$)	684,500	51,900	30,000	561,500	1,327,900
	C _F (USD\$)	54,900	6,700	4,850	54,100	120,550
	C _F /M _w (USD\$/m ³)	0.78	0.10	0.07	0.77	1.7
	Relative cost (%)	45.5	5.3	3.9	43.2	
	Reduction (%)	75.6	75.0	88.3	69.2	74.6

499

500 It should be highlighted that the MED plant implementation together with the solar fields,
501 represent the higher relative C_F of the main equipment, concretely 3.2 and 2.5 USD\$ per m³
502 treated at the smallest scale, respectively (see Table 8). If the treatment capacity of the MED
503 plant is increased to 200 m³/day, these costs can be reduced to 0.78 and 0.77 USD\$ per m³
504 treated, following the same order. Also, the C_F of the diesel generator and biomass boiler can
505 be diminished considerably, 88.3 and 75.0% respectively. Thus, the total annual fixed costs
506 per m³ treated are reduced in 74.6%, i.e. from 6.7 USD\$ per m³ to 1.8 USD\$ per m³.

507 On the other hand, the breakdown of operating consumptions is summarized in Table 9. As
508 commented in previous sections, the costs were obtained considering 350 operating days per
509 year that correspond to 70·10³ m³ treated per year and 24/7 operating regime and were also
510 scaled from 10 m³/day to 200 m³/day. The operating and maintenance costs were obtained
511 taking into account the reagents and chemical consumptions shown in Section 3.3 The main
512 consumptions are also described in Table 9. The maintenance cost was considered as 2% of

513 annual fixed cost according (Papapetrou et al., 2017) and the staff costs were considered as
514 0.03 USD\$ per m³ treated (Kesieme et al., 2013). The chemicals and consumables taken into
515 account were: (i) Anti-fouling with a consumption of 0.01 L/h for 10 m³/day and 0.02 L/h
516 for 200 m³/day. The anti-fouling consumptions was provided by INERCO. This consumption
517 is only considered in the inlet to to the process. (ii) Diesel consumptions was considered 3.7
518 L/h for 12 kW_e for 10 m³/day and 5.9 L/h for 45.8 kW_e for 200 m³/day. The data of diesel
519 consumptions were obtained from Worldwide Power Products LLC, approximate the fuel
520 consumptions of a diesel generator based on the size of the generator; (iii) Oil consumptions
521 was considered that each 250 h of operation the oil must be changed 6.5L; (iv) Refrigerant
522 consumptions was considered that each 1,000 h of operation the refrigerant must be changed
523 8L; (v) the biomass consumption were calculated as 4.9 kg/h for 38,6 kW_{th} for 10 m³/h and
524 63.2 kg/h for 775 kW_{th} for 200 m³/h, (vi) and finally the Sulfamic acid 5% was considered
525 as acid cleaning once per year.

526 **Table 9**
527 Breakdown of operating costs for MED plant installed (10 m³/day) and scaled up (200
528 m³/day)

Operating costs	10 m ³ /day			200 m ³ /day		
	C _v	Relative cost	C _v /M _w	C _v	Relative cost	C _v /M _w
	USD\$	%	USD\$/m ³	USD\$	%	USD\$/m ³
Staff (0.03 USD\$/m ³) ^a	110	0.4	0.03	2,100	1.8	0.03
Maintenance (2% I ₀) ^b	5,100	18.2	1.46	26,400	22.4	0.39
Chemicals and consumables						
Anti-fouling (0.01 L/h)	950	3.4	0.27	1,900	1.6	0.03
Diesel consumptions						
Semi-industrial, 10 m ³ /day:						
12 kW _e consumption 3.7 L/h	12,800	45.6	3.7	20,600	17.5	0.29
MED plant scaled, 200 m ³ /day:						
45.8 kW _e consumption 5.9 L/h						
Oil (change each 250 h, 6.5L)	1,350	4.8	0.38	3,000	2.6	0.04
Refrigerant (change each 1000 h, 8L)	250	0.9	0.07	500	0.4	0.007
Biomass: Pellets	7,400	26.4	2.1	63,000	53.6	0.9

<u>Semi-industrial, 10 m³/day:</u>						
38,6 kW _{th} consumption 4.9 kg/h						
<u>MED plant scaled, 200 m³/day:</u>						
775 kW _{th} consumption 63.2 kg/h						
Sulfamic Acid 5% (once per year)	75	0.3	0.02	75	0.06	0.001
TOTAL	28,035		8.0	117,575		1.7
^a Kesieme et al., 2013, ^b Papapetrou et al., 2017						

529

530 The diesel and biomass consumptions together with the maintenance, represent the most
531 important part of the operating costs associated with the treatment both at small (10 m³/day)
532 and large scale (200 m³/day). Previously, the highest cost was the diesel consumption, 3.7
533 USD\$/m³, which represents 45.6% of the total operating costs, followed by the pellets
534 consumption (2.1 USD\$/m³, 26.4 % relative cost) and maintenance (1.48 USD\$/m³, 18.2%
535 relative cost). However, the order changes at large scale (from 200 to 5,000 m³/day), where
536 the pellets consumption presents by far the highest relative cost (0.9 USD\$/m³, 53.6%),
537 followed by maintenance (0.39 USD\$/m³, 22.4%) and diesel consumption (0.29 USD\$/m³,
538 17.5%). The absolute increase in the diesel consumption due to the scaling up of the solar
539 water treatment system is much lower than the absolute increase in the pellets consumption.
540 Antifouling chemicals and oil for the electric generator represent about a 4% relative cost
541 each at small-scale and about 2% each at large-scale while staff salaries and sulfamic acid
542 consumption present almost negligible costs regardless of the scale. The solar water treatment
543 system scaling up allows a reduction of 78.7% in the total operating costs, which diminished
544 from 8.0 USD\$ per m³ treated for small scale to 1.7 USD\$ per m³ treated for large scale.
545 The cost of distilled water produced by the MED plant, SCOW, varies from 15.0 USD\$/m³
546 for the 10 m³/day production capacity to 3.2 USD\$/m³ when this variable is increased to 200
547 m³/day, which is equivalent to a 76.7% reduction (see Table 10). These high costs obtained

548 are clearly affected by the economy of scale and, mainly, due to use of diesel generator and
 549 biomass boiler, since the water treatment system is located in a remote arid area where the
 550 lack of electric grid and transport is a determinant factor.

551 As has been expressed during the whole study, the plant treatment capacity is extremely
 552 important for the SCOW. Therefore, a final study in which the relationship between these
 553 two variables is analyzed was carried out and it is presented in Fig. 5 and Table 10. These
 554 costs were calculated following the same sequence explained in Section 3.3. The highest cost
 555 reduction was observed in the case exposed above, i.e. when the MED production capacity
 556 was increased from 10 to 200 m³ per day, resulting in 76.7% SCOW reduction. The next
 557 analyzed level was 500 m³/day, which represented 37.1% SCOW improvement with respect
 558 to the previous case while varying from 500 m³/day to 1,000 m³/day resulted in 20.2% SCOW
 559 decrease. Thus, increasing the MED treatment capacity always results in the improvement of
 560 the SCOW. However, this improvement gets lower with each MED treatment capacity
 561 increase so that, finally, it becomes negligible.

562 **Table 10**
 563 The SCOW and reduction percentage achieved for different treatment capacities.

Treatment capacity (m ³ /day)	SCOW (USD\$/m ³)	Reduction percentage (%)
10	15.0	
200	3.20	76.7
500	2.20	85.3
1,000	1.76	88.3
2,500	1.40	90.7
5,000	1.25	91.6

564

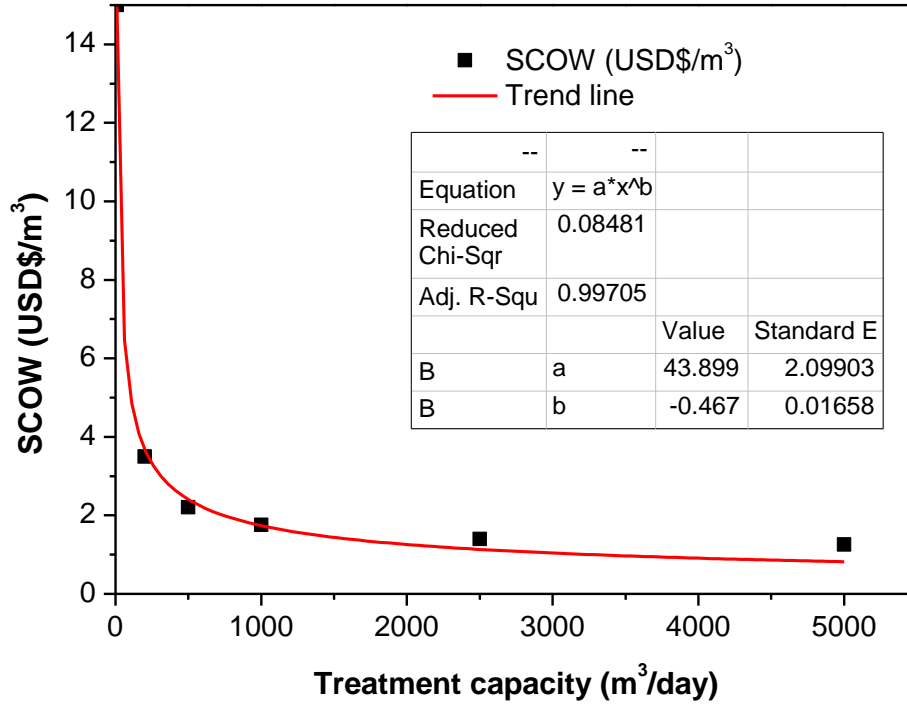


Fig. 5. Simplified Cost of Water (SCOW) versus treatment capacity (m³/day).

565

566 **4. Conclusions**

567 This paper presents the simulation of a MED pilot plant located in a remote community of
 568 the north of Chile (Taltape) that will be used to improve its agricultural activity and for
 569 domestic and hygiene purposes. From the operation of this plant, it has been demonstrated
 570 that the water treatment process allows diminishing As and B in 99% and 95%, respectively.
 571 The water treatment system will be coupled to a static solar thermal field to make it more
 572 sustainable taking advantage of the high solar radiation of the location. The whole system
 573 has been simulated along a whole year using meteorological data from Taltape in order to
 574 assess the solar operation of the water treatment plant and determine the use of a biomass
 575 boiler as a backup when the solar radiation is not available. An annual solar fraction of 46.6%
 576 and a total fresh water production with the MED operating with solar energy of 1,690 m³
 577 have been obtained, which make a total of 2,823 hours of exclusive solar operation. It means

578 that the needs of the community can be fully covered during most of the year with the solar
579 field, making a higher use of the biomass boiler (up to 48%) from May to August.
580 An economic assessment has been also performed in order to study the water costs of the
581 MED pilot plant and they scaled up to 5,000 m³/day. The cost of distilled water produced
582 by the MED plant varied from 15.0 USD\$/m³ for the 10 m³/day production capacity to 1.25
583 USD\$/m³ when this variable is increased to 5,000 m³/day, which is equivalent to a 91.6%
584 reduction. It was found that the MED plant implementation and solar fields represent the
585 higher relative annual fixed cost of the main equipment while the diesel and biomass
586 consumptions together with the maintenance represent the most important part of the
587 operating costs.

588

589

590 **Acknowledgments**

591 PhD. Lorena Cornejo Ponce wishes to thank the Region Government of Arica&Parincota
592 (FIC Taltape BIP code 30158422-0). PhD. Sara Miralles-Cuevas wishes to thank the Solar
593 Energy Research Center for her post-doctoral position in Arica, Chile, under SERC-Chile,
594 FONDAP project (reference: 15110019). PhD. Alejandro Cabrera wishes to thank his post-
595 doctoral position at University of Tarapacá. Patricia Palenzuela wishes to thank funding
596 support from the Spanish Ministry of Economy and Competitiveness and ERDF funds under
597 the National R+D+I Plan Project DPI2014-56364-C2-2-R.

598

599

600

601 **References**

602 Abejón, A., Garea, A., Irabien, A., 2015. Arsenic removal from drinking water by reverse
603 osmosis: Minimization of costs and energy consumption, *Separation and Purification*
604 *Technology* 144, 46-53.

605 Andrés-Mañas, J.A., Palenzuela, P., Cornejo, L., Alarcón-Padilla, D.C., Acién, G., Zaragoza,
606 G., 2017. Preliminary evaluation of the use of vacuum membrane distillation for the
607 production of drinking water in Arica (Chile), *Desalination & Water Treatment* 61, 160-169.

608 Bhattacharjee, P., Chatterjee, D., Singh, K., Giri, A., 2013. Systems biology approaches
609 to evaluate arsenic toxicity and carcinogenicity: an overview. *Int. J. Hyg. Environ. Health.*
610 216, 574–586.

611 Bick, A., Oron, G., 2005. Post-treatment design of seawater reverse osmosis plants: Boron
612 removal technology selection for potable water production and environmental control,
613 *Desalination* 178, 233–246.

614 Bundschuh, J., Litter, M., Ciminelli, V.S.T., Morgada, M.E., Cornejo, L., Hoyos, S.G.,
615 Hoinkis, J., Alarcón-Herrera, M.T., Armienta, M.A., Bhattacharya, P., 2010. Emerging
616 mitigation needs and sustainable options for solving the arsenic problems of rural and isolated
617 urban areas in Latin America - A critical analysis. *Water Research* 44 (19), 5828-5845.

618 Choong, T.S.Y., Chuah, T.G., Robiah, Y., Gregory Koay, F.L., Azni, I., 2007. Arsenic
619 toxicity, health hazards and removal techniques from water: an overview, *Desalination* 217
620 (1-3), 139-166.

621 Chorak, A., Palenzuela, P., Alarcón-Padilla, D.C., Abdellah, A.B., 2017. Experimental
622 characterization of a multi-effect distillation system coupled to a flat plate solar collector
623 field: empirical correlations, *Applied Thermal Engineering* 120, 298-313.

624 Couper, J.R., 2002. Process Engineering Economics, Chapter 4, page 70, CRC Press Ed.

625 Darwish, M., Hassan, A., Mohtar, R., 2013. Toward Implementing HH the Amir
626 Declaration of 2% Electricity Generation by Solar Energy in 2020, Energy and Power
627 Engineering 5, 245-258.

628 Decreto Supremo 143/2009. Normas de calidad primaria para las aguas continentales
629 superficiales aptas para actividades de recreación con contacto directo
630 (<https://www.leychile.cl/Navegar?idNorma=288386>).

631 Decreto Supremo 144/2009. Normas de calidad primaria para la protección de las aguas
632 marinas y estuarinas aptas para actividades de recreación con contacto directo
633 (<https://www.leychile.cl/Navegar?idNorma=1001042>).

634 Directive 98/83/EC. European Union, Council Directive 98/83/EC on the quality of water
635 intended for human consumption.

636 El-Dessouky, H., Ettouney, H., 2002. Fundamentals of Salt Water Desalination, 1^a ed.
637 Amsterdam, The Netherlands: ELSEVIER SCIENCE B.V, 2002.

638 El-Nashar, A.M. and Ishii, K., 1985. Abu Dhabi solar distillation plant, Desalination 52, 217-
639 234.

640 El-Nashar, A.M., Qamhiyeh, A.A., 1995. Simulation of the steady-state operation of a multi-
641 effect stach seawater distillation plant, Desalination 101, 231-243.

642 Fernández-Izquierdo, P., García-Rodríguez, L., Alarcón-Padilla, D., Palenzuela, P., Martín-
643 Mateos, I., 2012. Experimental analysis of a multi-effect distillation unit operated out of
644 nominal conditions, Desalination 284, 233-237.

645 GLASS Report, 2014. UN-Water Global Analysis and Assessment of Sanitation and
646 Drinking-Water GLAAS Report.

647 Hanel, M., Escobar, R., 2013. Influence of solar energy resource assessment uncertainty in
648 the levelized electricity cost of concentrated solar power plants in Chile, *Renewable Energy*
649 49, 96-100.

650 Hilal, N., Kim, G.J., Somerfield, C., 2011. Boron removal from saline water: A
651 comprehensive review, *Desalination* 273, 23–35.

652 Hong-Jie, S., Bala, R., Bing, W., Jun, L., Li-Ping, P., Lena, M., 2014. Arsenic and selenium
653 toxicity and their interactive effects in humans. *Environ. Int.* 69, 148–158.

654 Kesieme, U.K., Milne, N., Aral, H., Cheng, C.Y., Duke, M., 2013. Economic analysis of
655 desalination technologies in the context of carbon pricing, and opportunities for membrane
656 distillation, *Desalination* 323, 66–74, <http://dx.doi.org/10.1016/j.desal.2013.03.033>.

657 Li, C., Goswami, Y., Stefanakos, E., 2013. Solar assisted sea water desalination: a review,
658 *Renew. Sust. Energ. Rev.* 19, 136-163.

659 López, D.L., Bundschuh, J., Birkle, P., Armienta, M.A., Cumbal, L., Sracek, O., Cornejo,
660 L. , Ormachea, M., 2012. Arsenic in volcanic geothermal fluids of Latin America, *Science*
661 *of the Total Environment* 429, 57–75.

662 Mohtar, R. and Darwish, M., 2013. Prime Energy Challenges for Operating Power Plant in
663 GCC, *Energy and Power Engineering* 5, 109-128.

664 Öztürk, N., Kavak, D., Köse, T.E., 2008. Boron removal from aqueous solution by reverse
665 osmosis, *Desalination* 223, 1–9.

666 Palenzuela, P., Hassan, A.S., Zaragoza, G., Alarcón-Padilla, D.C., 2014. Steady-state model
667 for multi-effect distillation case study: Plataforma Solar de Almería MED pilot plant,
668 Desalination 337, 31-42.

669 Palenzuela, P., Alarcón-Padilla, D.C., Zaragoza, G., 2016. Experimental parametric analysis
670 of a solar pilot-scale multi-effect distillation plant, Desalination & Water Treatment 57,
671 23097-23109.

672 Papapetrou, M., Cipollina, A., La Commare, U., Micale, G., Zaragoza, G., Kosmadakis, G.,
673 2017. Assessment of methodologies and data used to calculate desalination costs,
674 Desalination 419, 8-19.

675 Seider W.D., Seader J.D., Lewin D.R., 2004. Product and Process Design Principles:
676 Synthesis, Analysis and Evaluation, 2nd Ed, Wiley.

677 Valenzuela, C., Mata-Torres, C., Cardemil, J.M., Escobar, R.A., 2017. CSP+PV hybrid solar
678 plants for power and water cogeneration in northern Chile, Solar Energy 157, 713-726.

679 Wang, Q., Zhang, G.S., Chen, H., Wang, P., 2016. Enhanced As(III) removal at low
680 concentrations by the combined pre-oxidation and nanofiltration membrane process,
681 Desalination and Water Treatment 57 (59), 28947-28956.

682 WHO, 2016. Evaluations of the Joint FAO/WHO Expert Committee on Food Additives
683 (JECFA): arsenic data. <http://www.who.int/mediacentre/factsheets/fs372/en/>

684 WHO and UNICEF, 2017. Progress on drinking water, sanitation and hygiene: 2017 update
685 and SDG baselines. Geneva: World Health Organization (WHO) and the United Nations
686 Children's Fund (UNICEF), 2017. Licence: CC BY-NC-SA 3.0 IGO. ISBN 978-92-4-
687 151289-3.

688 Yang, Y., Lior, N., 2006. Performance analysis of combined humidified gas turbine power
689 generation and multi-effect thermal vapour compression desalination systems Part1: the
690 desalination unit and its combination with a steam-injected gas turbine power system,
691 Desalination 196, 84–104.

692 Yunus, M., Sohel, N., Kumar Hore, S., Rahman, M., 2011. Arsenic exposure and adverse
693 health effects: a review of recent findings from arsenic and health studies in Matlab,
694 Bangladesh. Kaohsiung. J. Med. Sci. 27, 371–376.